Published in final edited form as:
Mol Cancer Ther. 2010 May ; 9(5): 1169–1179. doi:10.1158/1535-7163.MCT-09-1207.

Anticancer efficacy of a difluorodiarylidenyl piperidone (HO-3867) in human ovarian cancer cells and tumor xenografts

Karuppaiyah Selvendiran[1,*], **Liyue Tong**[1,*], **Anna Bratasz**[1], **M. Lakshmi Kuppusamy**[1], **Shabnam Ahmed**, **Yazhini Ravi**, **Nancy J. Trigg**[1], **Brian K. Rivera**[1], **Tamás Kálai**[3], **Kálmán Hideg**[3], and **Periannan Kuppusamy**[1,2]

[1]Department of Internal Medicine, Davis Heart and Lung Research Institute, The Ohio State University, Columbus, Ohio

[2]Comprehensive Cancer Center, The Ohio State University, Columbus, Ohio

[3]Institute of Organic and Medicinal Chemistry, University of Pécs, Pécs, Hungary.

Abstract

The purpose of this study was to evaluate the anticancer potency and mechanism of a novel difluorodiarylidenyl piperidone (H-4073) and its N-hydroxypyrroline modification (HO-3867) in human ovarian cancer. Studies were performed using established human ovarian cancer cell lines (A2870, A2780cDDP, OV-4, SKOV3, PA-1 and OVCAR3), as well as in a murine xenograft tumor (A2780) model. Both compounds were comparably and significantly cytotoxic to A2780 cells. However, HO-3867 demonstrated a preferential toxicity towards ovarian cancer cells, while sparing healthy cells. HO-3867 induced G2/M cell-cycle arrest in A2780 cells by modulating cell-cycle regulatory molecules p53, p21, p27, cdk2 and cyclin, and promoted apoptosis by caspase-8 and caspase-3 activation. It also caused an increase in the expression of functional Fas/CD95 and decreases in STAT3 (Tyr705) and JAK1 phosphorylation. There was a significant reduction in STAT3 downstream target protein levels including Bcl-xL, Bcl-2, survivin, and vascular endothelial growth factor (VEGF), suggesting that HO-3867 exposure disrupted the JAK/STAT3 signaling pathway. In addition, HO-3867 significantly inhibited the growth of the ovarian xenografted tumors in a dosage-dependent manner without any apparent toxicity. Western-blot analysis of the xenograft tumor tissues showed that HO-3867 inhibited pSTAT3 (Tyr705 and Ser727) and JAK1 and increased apoptotic markers cleaved caspase-3 and PARP. HO-3867 exhibited significant cytotoxicity towards ovarian cancer cells by inhibition of the JAK/STAT3-signaling pathway. The study suggested that HO-3867 may be useful as a safe and effective anticancer agent for ovarian cancer therapy.

Keywords

ovarian cancer; diarylidenyl piperidone; JAK/STAT3; curcumin; nitroxide

Introduction

Ovarian cancer is the second most commonly diagnosed gynecological malignancy among women in the United States (1,2). The current standard of care includes primary surgical cytoreduction followed by administration of cisplatin or cisplatin in combination with taxanes (3). Long-term administration of cisplatin has been shown to result in the development of

Correspondence: Periannan Kuppusamy, PhD, The Ohio State University, 420 West 12th Avenue, Room 114, Columbus, OH 43210. Phone: 614-292-8998; Fax: 614-292-8454; kuppusamy.1@osu.edu.
*Equal contribution

chemotherapeutic drug resistance in the cancer cell population(4,5). An increase in the cisplatin resistance of ovarian tumors requires the administration of larger doses of the drug that may lead to debilitating side effects, including severe multi-organ toxicities (6). Many chemotherapeutic drugs induce the production of reactive oxygen species (ROS), which are toxic to both cancerous and healthy cells. To reduce the side effects of chemotherapy and improve the quality of life, the majority of cancer patients use antioxidants in combination with conventional therapies. Unfortunately, adding antioxidants adjunctively may compromise the efficacy of these conventional therapeutic strategies (7).

Signal-transducer and activator of transcription 3 (STAT3), has been implicated in the pathogenesis of a variety of human malignancies including head and neck cancer, myeloma, prostate cancer, breast cancer, colon cancer, and ovarian cancer (8–11). Activation of STAT3 can be accomplished by the Janus kinases (JAKs, including TYK2), activated epidermal growth factor receptor (EGFR), and Src kinase (12). STAT3 is constitutively activated in many tumor types, and this activation promotes acceleration of cell proliferation, upregulation of survival factors, and activation of anti-apoptotic proteins. This imparts cellular resistance to chemotherapy by inhibiting apoptosis in epithelial malignancies, including ovarian cancer (13,14). Because of its important role in oncogenesis, STAT3 has attracted much attention as a potential pharmacologic target for cancer treatment (11,15,16).

Curcumin, a beta-diketone constituent of turmeric derived from the rhizome of the plant *Curcuma longa*, has been shown to inhibit the many cellular signaling pathways, including the JAK-STAT pathway, and to downregulate the expression of many tumor-promoting downstream proteins and signaling cascades (16,17). Curcumin has been shown to have antiproliferative and antiangiogenic activities in several tumors, including ovarian cancer (18,19). However, the clinical use of curcumin has been limited due to its low anticancer activity and poor absorption. Recently, a novel class of curcumin analogs, diarylidenyl piperidones (DAPs), has been developed by incorporating a piperidone link to the beta-diketone structure and fluoro-substitutions on the phenyl groups (20). The DAP compounds, in general, were more effective than curcumin in inhibiting the proliferation of a variety of cancer cell lines (21). EF24, one of the DAP compounds with *ortho*-fluorinated phenyl groups exhibited potent anticancer efficacy *in vitro* when tested using breast cancer (21), colon cancer (22), and ovarian epithelial cancer (23) cell lines. Subsequently, we observed that H-4073 (Figure 1), a *para*-fluorinated variant, was more potent than EF24 in inducing cytotoxicity to ovarian cancer cells (24,25).

A nonspecific cytotoxic compound may have side effects caused by damage to normal cells. For example, many chemotherapeutic agents act by producing free radicals, which may increase oxidative stress in normal cells (26,27). To minimize this toxicity, there is a need to use detoxicants, such as antioxidants, that can differentiate between healthy and cancerous cells and selectively protect the healthy cells by scavenging free radicals (28,29). It has been shown that nitroxides, a class of small-molecular-weight heterocyclic molecules containing “>NO”, and hydroxylamines, the one-electron-reduced form of nitroxides characterized by “>NOH”, preferentially scavenge oxygen radicals in cells that have normal oxygenation or redox status (30,31). Hydroxylamines are referred to as “pro-nitroxides”, as the hydroxylamine form of the molecules exist in equilibrium with the nitroxide form in well-oxygenated tissues (30,31). Most tumors are hypoxic in nature, and their cellular environment is more reducing (for example, thiol-rich) when compared to healthy cells (32,33). This differential aspect between normal and cancerous cells has led us to the design of HO-3867 (Figure 1) which would have both anticancer and antioxidant properties (25). Hence, the specific goals of the present study were: (i) to determine the anticancer efficacy of HO-3867 towards cancerous and a noncancerous (control) cell lines; (ii) to derive mechanistic insights into the action of HO-3867; and (iii) determine whether or not HO-3867 would significantly inhibit tumor

growth in an *in vivo* model of ovarian cancer. The studies were conducted using human ovarian cancer cell lines and a murine xenograft model of ovarian cancer. The results showed a preferential toxicity of HO-3867 towards ovarian cancer cells, and suppression of tumor growth through inhibition of the JAK/STAT3 pathway both *in vitro* and *in vivo*.

Materials and methods

Chemicals

Curcumin, superoxide dismutase (SOD), 6-carboxy-2',7'-dichlorodihydrofluorescein diacetate, diacetoxy-methyl ester (H_2DCF-DA), 3-(4,5-dimethylthiazol-2-yl)-2,5-diphenyltetrazolium bromide (MTT), and antibodies against actin were obtained from Sigma (St. Louis, MO). 5-diethoxyphosphoryl-5-methyl-1-pyrroline-*N*-oxide (DEPMPO) was from Radical Vision (Jerome-Marseille, France). Cell-culture medium (RPMI 1640), fetal-bovine serum (FBS), antibiotics, sodium pyruvate, trypsin, and phosphate-buffered saline (PBS) were purchased from Gibco (Grand Island, NY). Polyvinylidene fluoride (PVDF) membrane and molecular-weight markers were obtained from Bio-Rad (Hercules, CA). Antibodies against poly-adenosine diphosphate ribose polymerase (PARP), cleaved caspase-3, caspase-7, caspase-8, STAT3, phospho-STAT3 (Tyr705), JAK1, Bcl-xL, and phospho-JAK1 (Tyr1022/1023) were purchased from Cell Signaling Technology (Beverly, MA). Antibodies specific for cyclin A, cyclin D1, Cdk2, p53, p21, p27, Fas/CD95, FasL, Bcl-2 and ubiquitin were purchased from Santa Cruz Biotechnology (Santa Cruz, CA). Enhanced chemiluminescence (ECL) reagents were obtained from Amersham Pharmacia Biotech (GE Healthcare-Piscataway, NJ). All other reagents, of analytical grade or higher, were purchased from Sigma-Aldrich, unless otherwise noted.

Synthesis of H-4073 and HO-3867

Melting points were determined with a Boetius micro-melting point apparatus and are uncorrected. Elemental analyses (C, H, N, S) were performed on a Fisons EA 1110 CHNS elemental analyzer. Mass spectra were recorded on Thermoquest Automass Multi and VG TRIO-2 instruments the EI mode. ^{1}H NMR spectra were recorded with a Varian UNITYINOVA 400 WB spectrometer. Chemical shifts are referenced to Me_4Si. Measurements were run at 298K probe temperature in a $CDCl_3$ solution. Flash column chromatography was performed on a Merck Kieselgel 60 (0.040–0.063 mm). Qualitative TLC was carried out on commercially prepared plates (20 × 20 × 0.02 cm) coated with Merck Kieselgel GF_{254}. All chemicals were purchased from Aldrich. Compound HO-350 was prepared as described earlier (34).

(3*E*,5*E*)-3,5-Bis(4-fluorobenzylidene)piperidin-4-one (H-4073)—A solution of 4-fluorobenzaldehyde (2.48 g, 20.0 mmol) and 4-piperidone hydrate hydrochloride (1.53 g, 10.0 mmol) was allowed to stay in glacial acetic acid (saturated with HCl gas previously) for 2 days. The precipitated yellow solid was filtered, washed with Et_2O (30 ml) and the yellow hydrochloride salt 2.50 g, (72%, melting point 212–214°C) was air-dried and used in the next step without further purification. For analytical characterization 300 mg of the salt was dissolved in water (10 ml) and basified by addition of 250 mg K_2CO_3 and extracted with $CHCl_3$ (3×10 ml). The combined extracts were dried ($MgSO_4$), filtered and evaporated to give yellow solid R_f: 0.43 ($CHCl_3$/Et_2O, 2:1). MS (EI, 70 eV): m/z (%): 311 (M^+, 73) 282 (43), 148 (36), 133(100). Anal Calcd. for: $C_{19}H_{15}F_2NO$: C 73.30; H 4.86; N 4.50. Found: C 73.19; H 4.83; N 4.32. ^{1}H NMR (399.9 MHz, DMSO-d_6): δ 4.38 (s, 4 H), 7.26 (t, 4 H), 7.48 (m, 4H), 7.81 (s, 2H).

1-[(1-Oxyl-2,2,5,5-tetramethyl-2,5-dihydro-1H-pyrrol-3-yl)methyl]-(3*E*,5*E*)-3,5-Bis(4-fluorobenzylidene)piperidin-4-one (HO-3867)—A mixture of H-4073 HCl salt

(1.73 g, 5.0 mmol), K_2CO_3 (1.38g, 10.0 mmol) in acetonitrile (20 ml) was stirred at room temperature for 30 min, then allylic bromide, and HO-350 (1.28 g, 5.5 mmol) were added dissolved in acetonitrile (5 ml) and the mixture was stirred and refluxed till the consumption of the starting materials (~3 h). After cooling, the inorganic salts were filtered off on sintered glass filter, washed with $CHCl_3$ (10 ml), the filtrate was evaporated and the residue was partitioned between $CHCl_3$ (20 mL) and water (10 ml). The organic phase was separated, the aqueous phase was washed with $CHCl_3$ (20 ml), the combined organic phase was dried ($MgSO_4$), filtered and evaporated. The residue was purified by flash column chromatography (Hexane/EtOAc) to give the title compound as a deep yellow solid 1.36 g (59%), R_f: 0.57 (Hexane/EtOAc, 2:1), mp 142–144 °C. MS (EI, 70 eV): m/z (%): 463 (M^+, 12) 433 (20), 324 (40), 310 (43), 133(100). ESR: a_N = 14.9 G. Anal Calcd. for: $C_{28}H_{29}F_2N_2O_2$: C 72.55; H 6.31; N 6,04. Found: C 72.54; H 6.23; N 6.04.

To achieve the *N*-hydroxy compound HCl salt, HO-3867 (1.0 g) was dissolved in EtOH (20 ml, saturated with HCl gas previously) and refluxed for 30 min, then the solvent was evaporated off and the procedure was repeated till the disappearance of the EPR triplet line to give the HCl salt. A detailed report on the synthesis and structure-activity relationship of a number of DAP derivatives will be published separately (35). Stock solutions of the compounds were freshly prepared in dimethylsulfoxide (DMSO).

Cell lines and cultures

The A2780 human epithelial ovarian cancer cell line was used for most parts of the study. Other ovarian cancer cell lines used (SKOV3, OVCAR3, A2780R and OV4), as were normal human ovarian surface epithelial (hOSE; ScienCell Ovarian Cell System) cells were grown in RPMI 1640 and DMEM medium supplemented with 10% FBS, 2% sodium pyruvate, 1% penicillin and 1% streptomycin. Cells were grown in a 75-mm flask to 70% confluence at 37°C in an atmosphere of 5% CO_2 and 95% air. Cells were routinely trypsinized (0.05% trypsin/EDTA) and counted using an automated counter (NucleoCounter, New Brunswick Scientific, Edison, NJ).

Cell viability by MTT assay

Cell viability was determined by a colorimetric assay using MTT. In the mitochondria of living cells, yellow MTT undergoes a reductive conversion to formazan, producing a purple color. Cells, grown to ~80% confluence in 75-mm flasks, were trypsinized, counted, seeded in 96-well plates with an average population of 7,000 cells/well, incubated overnight, and then treated with curcumin, H-4073, or HO-3867 for 24 h. All experiments were done using 8 replicates and repeated at least three times.

Cell proliferation by clonogenic assay

Cell survival was assessed by clonogenic assay. Cells at ~80% confluence were trypsinized, rinsed, seeded onto 60-mm dishes (5×10^4 cells per dish), grown for 24 h at 37°C, and treated afterward with H-4073 or HO-3867 for 24 h. Untreated cells served as controls. After treatment, the cells were washed twice with PBS, trypsinized, counted, and plated in 60-mm dishes in triplicate and incubated for an additional 7 days. The colonies were then stained with crystal violet (in ethyl alcohol) and counted using an automated colony counter (ColCount, Oxford Optronix, Oxford, UK). Each experiment was repeated at least five times.

Cell-cycle analysis

Cells were treated with HO-3867 (10 μM) for 24 h, trypsinized, washed in PBS, and fixed in an ice-cold 75% ethanol/PBS solution. The DNA was labeled with propidium iodide. Cells

were sorted by flow cytometry, and cell-cycle profiles were determined using ModFit LT software (Becton Dickinson, San Diego, CA).

Immunoblot analysis

Cells in RPMI 1640 medium were treated with DMSO (control) or HO-3867 (10 μM) for 24 h. Equal volumes of DMSO (0.1% v/v) were present in each treatment. Following treatment, the cell lysates were prepared in nondenaturing lysis buffer containing 10-mM Tris-HCl (pH 7.4), 150-mM NaCl, 1% Triton X-100, 1-mM EDTA, 1-mM EGTA, 0.3-mM phenylmethylsulfonyl fluoride, 0.2-mM sodium orthovanadate, 0.5% NP40, 1-μg/ml aprotinin, and 1-μg/ml leupetin. The lysates were centrifuged at 10,000×g for 20 min at 4°C, and the supernatant was separated. The protein concentration in the lysates was determined using a Pierce detergent-compatible protein assay kit. For Western blotting, 25 to 50 μg of protein lysate per sample was denatured in 2× SDS-PAGE sample buffer and subjected to SDS-PAGE on a 10% tris-glycine gel. The separated proteins were transferred to a PVDF membrane and blocked with 5% nonfat milk powder (w/v) in TBST (10-mM Tris, 10-mM NaCl, 0.1% Tween 20) for 1 h at room temperature or overnight at 4°C. The membranes were then incubated with the primary antibodies. The bound antibodies were detected with horseradish peroxidase (HRP)-labeled sheep anti-mouse IgG or HRP-labeled donkey anti-rabbit IgG using an enhanced chemiluminescence detection system (ECL Advanced kit). Protein expressions were determined using Image Gauge v. 3.45 software.

Ovarian cancer tumor xenografts in mice

Cultured A2780 cancer cells (2×10^6 cells in 60 μl of PBS) were subcutaneously (s.c.) injected into the back of 6-week-old BALB/c nude mice from the National Cancer Institute. 5 to 7 days later, when the tumors reached 3–5 mm in diameter, the mice were divided (n=9 / group) in a manner to equalize the mean tumor diameter among the groups. The control group was given a normal diet (no treatment) while the experimental groups were treated using the DAP compounds mixed with the animal feed (Harlan Teklad) at 3 different levels (25, 50, and 100 ppm). The doses were chosen based on an initial dose-response study optimized to produce an observable effect on tumor growth. The size of the tumor was measured two times per week using a digital Vernier caliper. The tumor volume was determined from the orthogonal dimensions (d_1, d_2, d_3) using the formula $(d_1 \times d_2 \times d_3) \times \pi/6$. Thirty five days after the beginning of HO-3867 treatment, the mice were sacrificed, and the tumors were resected. The tumor tissues were then subjected to immunoblot analysis.

Data analysis

The statistical significance of the results was evaluated using ANOVA and a Student's t-test. A p value of less than 0.05 was considered significant.

Results

HO-3867 is cytotoxic to A2780, and other ovarian cancer cell lines

The cytotoxic effects of H-4073 and HO-3867 were evaluated and compared with that of curcumin in A2780 and other established human ovarian cancer cell lines. Figure 1A compares the effect of curcumin, H-4073, and HO-3867 on the viability of A2780 cells. While all three compounds showed a dose-dependent cytotoxicity, H-4073 and HO-3867 exhibited significantly higher toxicity when compared to curcumin. The results further indicated that the cytotoxic effects of HO-3867 and H-4073 on A2780 cells were comparable, suggesting that the introduction of the N-hydroxypyrroline moiety in HO-3867 did not compromise the cytotoxic effect of HO-3867 against A2780 cells. We next performed clonogenic assays to study the effectiveness of H-4073 and HO-3867 on the proliferation of A2780 cells. Both

compounds demonstrated a dose-dependent reduction in the number of colonies (Figure 1B) suggesting that the compounds are equally potent in inhibiting cell proliferation. We further tested the cytotoxicity of H-4073 and HO-3867 in a number of other well-established human ovarian cancer cell lines including a cisplatin-resistant derivative of A2780 (A2780R), PA-1, SKOV3, OV4, and OVCAR3. The results (Figure 1C) showed that both H-4073 and HO-3867 were equally and significantly toxic to the tested cell lines. We then tested the effect of HO-3867 exposure on hOSE cells, which are noncancerous control cells derived from human ovarian surface epithelial cells. As shown in Figure 1D, no significant cytotoxicity to hOSE cells was observed for up to 10-μM concentration of HO-3867. However, treatment with 20-μM H-4073 or HO-3867 showed significant cytotoxicity to hOSE cells. Taken together, the cellular viability studies demonstrated that both H-4073 and HO-3867 were comparably and significantly effective in inducing cytotoxicity in A2780 and other ovarian cancer cell lines; however, HO-3867 was significantly less toxic to noncancerous ovarian surface epithelial cells, when compared to H-4073.

HO-3867 induces G2/M cell-cycle arrest in A2780 cells

We next examined whether the growth inhibition of A2780 cells by HO-3867 was caused by cell-cycle arrest. Cells were treated with HO-3867 for 6, 12, or 24 h, fixed, and cell-cycle populations were determined by flow cytometry. The results showed that the percentages of the cell population in the G2/M and subG1 phases were significantly higher in the treatment group when compared to the untreated control group (Figure 2A, and 2B). We then determined the effect of HO-3867 on the cell-cycle regulatory molecules p53, p21, p27, cdk2 and cyclin A (Figure 2C) by Western blotting. The levels of p53, and p21 were significantly upregulated while cdk2 and cyclin-A levels were significantly decreased after treatment (Figure 2D). These results indicated that HO-3867 caused G_2/M cell-cycle arrest, at least in part, by modulating cell-cycle regulatory proteins.

HO-3867 induces apoptosis in A2780 cells

The arrest of cell-cycle progression in cancer cells is usually associated with concomitant activation of pro-apoptotic pathways. To determine whether HO-3867-induced cell-cycle arrest led to apoptosis, the expression of activated caspases were probed by Western blotting. The blots showed the activation of caspase-8, caspase-7, cleaved caspase-3, and PARP in A2780 cells treated with HO-3867 for 24 h (Figure 3A). The quantitative results of the immunoblots (Figure 3B) showed a significant increase in the level of these caspases in cells treated with HO-3867 when compared to untreated cells. We further determined the levels of caspase-8-associated death receptors such as Fas/CD95 and Fas-L. The data from the Fas/CD95 expression showed a clear increase in HO-3867-treated cells when compared to untreated group. However, no significant change was observed in Fas-L (*data not shown*).

HO-3867 inhibits the JAK/STAT3 pathway

The constitutive activation of STAT3 in ovarian cancer has been shown to regulate the expression of genes implicated in tumor-cell proliferation and survival (36,37). To determine whether the HO-3867-induced growth inhibition in A2780 cell was mediated by STAT3, we examined the level of phosphorylated STAT3 (pSTAT3) by Western blotting (Figure 4A). The pSTAT3 (Tyr705 and Ser727) levels were significantly decreased after treatment with 10 or 20-μM HO-3867 for 24 hours. Excessive Janus kinase (JAK) activity in tumor cells is one of the most common mechanisms for constitutive activation of STAT3. To examine whether HO-3867 exposure resulted in a decrease in STAT3 activation through JAK kinase inhibition, we measured the phosphorylated level of JAK1 after 24 hours of exposure to 10- or 20-μM HO-3867 (Figure 4A). In addition, we cross-checked the expression of these proteins using immunoprecipitation, and confirmed the decreased expression of pSTAT3 and pJAK1 with no

change in the total expression levels of these proteins. The data showed a substantial decrease in phospho-JAK1 (Tyr1022/1023) when compared to unexposed controls, suggesting that HO-3867 blocked the JAK/STAT3 pathway. Before proceeding to *in vivo* experiments, we confirmed the potent apoptosis-inducing effect of HO-3867 in four additional ovarian cancer cell lines, A2780R, SKOV3, OV4 and OVCAR3. Following HO-3867 treatment, all four cell lines clearly demonstrated caspase-3 and PARP cleavage, accompanied by a decrease in the expression levels of phosphorylated STAT3 and JAK1 (Figure 4B). The results suggested that induction of apoptosis and inhibition of JAK/STAT3 signaling could be caused by HO-3867 in human ovarian cancer cell lines.

HO-3867 down-regulates the STAT3 target proteins

To investigate the downstream consequences of STAT3 inhibition, Western blotting was performed to determine the protein levels of Bcl-xL, Bcl-2, survivin, VEGF, and cyclin D1 following 24-h exposure to HO-3867 at 10- and 20-μM concentrations. There was a clear reduction in Bcl-xL, Bcl-2, survivin, and VEGF levels, while no significant change in cyclin D1 level was observed (Figures 4C). Because these proteins are involved in anti-apoptotic (survivin, Bcl-2 and Bcl-xL), and angiogenic (VEGF) protein expressions, the downregulation of these proteins suggested profound antitumor potential of HO-3867 in ovarian cancer cells. The results clearly demonstrated the involvement of the STAT3 pathway in the growth inhibition of the A2780 ovarian cancer cells by HO-3867.

HO-3867 inhibits the growth of xenograft tumor in mice

Based on our *in vitro* results which showed significant cytotoxicity of HO-3867 to human ovarian cancer cell lines, we next evaluated the efficacy of HO-3867 in a human ovarian tumor xenograft grown in the back of mice. The mice were treated with HO-3867 and the tumor size was measured twice weekly for 5 weeks, as reported (10,15). A significant reduction in the tumor volume was observed in a dose-dependent manner; particularly the doses of 50 and 100 ppm were more effective when compared with vehicle-treated controls (Figure 5). We also measured the body weight and diet consumption of tumor-bearing animals. HO-3867-treated animals did not show any gross signs of toxicity and/or possible adverse side effects as measured by two profiles; body weight (Figure 5C) and diet consumption (Figure 5D). These results suggest *in vivo* antitumor efficacy of HO-3867 against ovarian tumor without any apparent signs of toxicity.

HO-3867 inhibits pSTAT3 and downregulates the STAT3-targeting proteins *in vivo*

We further analyzed the excised tumor tissue to determine whether HO-3867 inhibited the STAT3/JAK protein expression levels, as observed in the *in vitro* studies. In concert with the decreased expressions in both pSTAT3 Tyr705 and Ser727 levels, without affecting total STAT3, we observed a clear down-regulation of total JAK levels in tumor tissues. However we did not observe any significant change in pJAK levels in tumor tissues (Figure 6A). As for the target gene products of STAT3, we observed a clear decrease of cyclin D1, VEGF, Bcl-2 and Survivin levels in the HO-3867-treated tumors (Figure 6B). Interestingly we noticed a significant induction of cleaved caspase-3 and PARP, which is a known marker of apoptosis and a downstream target of activated caspase-3 (38) (Figure 6C & D), suggesting that HO-3867 induced apoptosis *in vivo*.

Discussion

The results of the present study established that the difluorodiarylidenyl piperidone, HO-3867, exhibits potent anticancer efficacy towards human ovarian cancer cells and xenograft tumors. HO-3867, which also incorporates an antioxidant function, exhibits substantially lower toxicity towards noncancerous cells. The mechanistic studies revealed that HO-3867 targets multiple

pathways, including altering the proteins involved in G2/M cell-cycle arrest, increased expression of Fas/CD95, downregulation of anti-apoptotic signals, and inhibition of the JAK/STAT3 pathway in both *in vitro* and *in vivo*.

Cell-cycle control plays a critical role in the regulation of tumor-cell proliferation. Many cytotoxic agents arrest cell cycle at the G1, S, or G2/M phase. In the present study, HO-3867 induced G2/M cell-cycle arrest in A2780 cells as evidenced by a significant increase in the p53, p21, and p27 protein levels. We also observed a significant reduction in Cdk2 and cyclin A levels. Previous studies have shown that the G2/M-phase progression is regulated by a number of Cdk/cyclins as well as Cdk inhibitors such as p21 and p27 (23). Hence, our results suggest that the HO-3867-induced G2/M cell-cycle arrest is mediated by the induction of p53 and p21 and downregulation of cyclin A and Cdk2.

Many curcumin derivatives induce apoptosis in cancer cells, but the mechanisms by which they do so differ (22,23). The death receptor–associated mechanism has been recently receiving much attention for the anticancer activity of curcumin derivatives (39,40). We observed that the death-receptor gene Fas/CD95 was activated in A2780 cells by HO-3867. We further observed that the expression level of TNF-R1, the receptor of TNF-α, was unchanged in the HO-3867-treated A2780 cells (*data not shown*). It has been reported that curcumin promoted TNF-α-induced apoptosis in a variety of cancer cells, but without a significant increase in the TNF-R1 expression level. Curcumin and curcumin analogs have also been shown to upregulate death receptor 5 (DR5) and FasL expression, thereby inducing apoptosis in human cancer cells (23,41). Thus, our results suggest a critical involvement of upregulated death-receptor super-family-mediated signals in the stimulation of A2780 apoptosis following HO-3867 exposure.

STAT3 has been shown to suppress the transcription of Fas/CD95 (42). This suggests the HO-3867-mediated downregulation of STAT3 expression, in both *in vitro* and *in vivo*, as a putative mechanism for increased Fas/CD95 expression. This is obvious from the substantial decrease in the level of Tyr705-phosphorylated STAT3, a major active form of activated STAT3. It is noteworthy that the expression level of Ser727-phosphorylated STAT3 was also clearly decreased *in vivo*. Because the Ser727 phosphorylation is also known to regulate the transcriptional activity of STAT3 (20,21), this attenuated phosphorylation is suggested to participate in the down-regulation of the transcriptional activity of STAT3 in the xenograft tumor treated with HO-3867. We also observed that HO-3867 caused a substantial inhibition of phospho-JAK1 (Tyr-1022/1023) suggesting that HO-3867 can inhibit the constitutive activation of STAT3, which may be caused, at least in part, by the inhibition of pJAK1. However, HO-3867 may also inhibit STAT3 activation through JAK2, Src, Erb2, and EGFR, which are known to be implicated in STAT3 activation as well. Additional studies are needed to explore these pathways.

Downstream proteins of STAT3 have been shown to regulate apoptosis and regulation in cancer cells. For example, Bcl-xL, Bcl-2, and survivin have been shown to suppress apoptosis, while c-myc and cyclin D1 have been shown to mediate proliferation (43,44). Because of the fact that STAT3 downregulating genes are all critically involved in the development of cancer aggressiveness, targeting STAT3 is considered a potential anticancer strategy. Furthermore, inhibition of STAT3 expression *in vivo* has provided deep insight into a new approach for the treatment of human tumors (16,45). In addition, inhibition of STAT3 activation has been shown to be valid in inducing significant apoptosis in both the mice model of melanoma xenografts and that of squamous cell carcinoma xenografts (8). The induction of apoptosis in tumor is another approach to limit their uncontrolled proliferation of tumor growth. In this process, activation of caspases is the central event (46). Once activated, the executioner caspases downstream of the cascade act on the key molecules inside the cells to orchestrate cell death. In the present study, we observed that HO-3867 clearly induces apoptotic death both *in vitro*

and *in vivo*, at least in part, due to activation of caspase-3 and cleavages of PARP. Cleavage of poly (ADP-ribose) polymerase by activated caspases is considered as a marker for apoptotic death (38). STAT3 is also known to protect cells from apoptosis through upregulation of Bcl-xL, Bcl-2 and survivin (15). The expression levels in all of these molecules downstream of STAT3 activation were clearly reduced in ovarian cancer cells by exposure to HO-3867, not only *in vitro* but also *in vivo* - even in mice given a low concentration (50 ppm) of HO-3867. This implies that induction of apoptosis may be an additional contributing factor in the HO-3867-mediated inhibition of ovarian tumor growth. However, further studies are essential to elucidate the mechanism of apoptosis induction by HO-3867.

In summary, we have investigated the anticancer efficacy of a novel curcuminoid compound, HO-3867, which inhibited ovarian tumor growth by inhibition of the JAK1/STAT3 signaling pathway. HO-3867 shows substantial promise for further development it as a potential agent for treating ovarian cancer.

Abbreviations

A2780	human ovarian cancer cell line
hOSE	human ovarian surface epithelial cell
DAP	diarylidenyl piperidone
JAK	Janus kinase
MTT	3-(4,5-dimethylthiazol-2-yl)-2,5-diphenyltetrazolium bromide
ROS	reactive oxygen species
STAT3	signal-transducer and activator of transcription 3

Acknowledgments

This work was supported by NIH grant CA102264 (PK), The Kaleidoscope of Hope Foundation grant (KS), and Hungarian Research Fund Grant OTKA K81123 (KH). The authors thank Shabnam Ahmad and Yazhini Ravi for their assistance with the Western-blot assays and Mária Balog for her help with the synthesis of the compounds.

REFERENCES

1. Jemal A, Siegel R, Ward E, et al. Cancer statistics, 2008. CA Cancer J Clin 2008;58:71–96. [PubMed: 18287387]
2. Ozols RF, Bookman MA, Connolly DC, et al. Focus on epithelial ovarian cancer. Cancer Cell 2004;5:19–24. [PubMed: 14749123]
3. Bristow RE, Chi DS. Platinum-based neoadjuvant chemotherapy and interval surgical cytoreduction for advanced ovarian cancer: a meta-analysis. Gynecol Oncol 2006;103:1070–1076. [PubMed: 16875720]
4. Harries M, Gore M. Part II: chemotherapy for epithelial ovarian cancer-treatment of recurrent disease. Lancet Oncol 2002;3:537–545. [PubMed: 12217791]
5. Harries M, Gore M. Part I: chemotherapy for epithelial ovarian cancer-treatment at first diagnosis. Lancet Oncol 2002;3:529–536. [PubMed: 12217790]
6. Borst P, Rottenberg S, Jonkers J. How do real tumors become resistant to cisplatin? Cell Cycle 2008;7:1353–1359. [PubMed: 18418074]
7. Raj MH, Abd Elmageed ZY, Zhou J, et al. Synergistic action of dietary phyto-antioxidants on survival and proliferation of ovarian cancer cells. Gynecol Oncol 2008;110:432–438. [PubMed: 18603286]
8. Yu H, Jove R. The STATs of cancer--new molecular targets come of age. Nat Rev Cancer 2004;4:97–105. [PubMed: 14964307]

9. Lu Y, Zhou J, Xu C, et al. JAK/STAT and PI3K/AKT pathways form a mutual transactivation loop and afford resistance to oxidative stress-induced apoptosis in cardiomyocytes. Cell Physiol Biochem 2008;21:305–314. [PubMed: 18441519]
10. Selvendiran K, Bratasz A, Tong L, Ignarro LJ, Kuppusamy P. NCX-4016, a nitroderivative of aspirin, inhibits EGFR and STAT3 signaling and modulates Bcl-2 proteins in cisplatin-resistant human ovarian cancer cells and xenografts. Cell Cycle 2008;7:81–88. [PubMed: 18196976]
11. Yang F, Van Meter TE, Buettner R, et al. Sorafenib inhibits signal transducer and activator of transcription 3 signaling associated with growth arrest and apoptosis of medulloblastomas. Mol Cancer Ther 2008;7:3519–3526. [PubMed: 19001435]
12. Clevenger CV. Roles and regulation of stat family transcription factors in human breast cancer. Am J Pathol 2004;165:1449–1460. [PubMed: 15509516]
13. Durrant D, Richards JE, Walker WT, Baker KA, Simoni D, Lee RM. Mechanism of cell death induced by cis-3, 4', 5-trimethoxy-3'-aminostilbene in ovarian cancer. Gynecol Oncol 2008;110:110–117. [PubMed: 18433847]
14. Trachootham D, Zhou Y, Zhang H, et al. Selective killing of oncogenically transformed cells through a ROS-mediated mechanism by beta-phenylethyl isothiocyanate. Cancer Cell 2006;10:241–252. [PubMed: 16959615]
15. Selvendiran K, Koga H, Ueno T, et al. Luteolin promotes degradation in signal transducer and activator of transcription 3 in human hepatoma cells: an implication for the antitumor potential of flavonoids. Cancer Res 2006;66:4826–4834. [PubMed: 16651438]
16. Bharti AC, Shishodia S, Reuben JM, et al. Nuclear factor-kappaB and STAT3 are constitutively active in CD138+ cells derived from multiple myeloma patients, and suppression of these transcription factors leads to apoptosis. Blood 2004;103:3175–3184. [PubMed: 15070700]
17. Kim HY, Park EJ, Joe EH, Jou I. Curcumin suppresses Janus kinase-STAT inflammatory signaling through activation of Src homology 2 domain-containing tyrosine phosphatase 2 in brain microglia. J Immunol 2003;171:6072–6079. [PubMed: 14634121]
18. Weir NM, Selvendiran K, Kutala VK, et al. Curcumin induces G2/M arrest and apoptosis in cisplatin-resistant human ovarian cancer cells by modulating Akt and p38 MAPK. Cancer Biol Ther 2007;6:178–184. [PubMed: 17218783]
19. Lin YG, Kunnumakkara AB, Nair A, et al. Curcumin inhibits tumor growth and angiogenesis in ovarian carcinoma by targeting the nuclear factor-kappaB pathway. Clin Cancer Res 2007;13:3423–3430. [PubMed: 17545551]
20. Adams BK, Ferstl EM, Davis MC, et al. Synthesis and biological evaluation of novel curcumin analogs as anti-cancer and anti-angiogenesis agents. Bioorg Med Chem 2004;12:3871–3883. [PubMed: 15210154]
21. Adams BK, Cai J, Armstrong J, et al. EF24, a novel synthetic curcumin analog, induces apoptosis in cancer cells via a redox-dependent mechanism. Anticancer Drugs 2005;16:263–275. [PubMed: 15711178]
22. Subramaniam D, May R, Sureban SM, et al. Diphenyl difluoroketone: a curcumin derivative with potent in vivo anticancer activity. Cancer Res 2008;68:1962–1969. [PubMed: 18339878]
23. Selvendiran K, Tong L, Vishwanath S, et al. EF24 induces G2/M arrest and apoptosis in cisplatin-resistant human ovarian cancer cells by increasing PTEN expression. J Biol Chem 2007;282:28609–28618. [PubMed: 17684018]
24. Tazi MF, Selvendiran K, Kuppusamy ML, et al. Evaluation of a novel class of fluorinated curcumin analogs for safe and targeted anticancer therapy (STAT). Free Radic Biol Med 2008;45:S56–S57.
25. Selvendiran K, Ahmed S, Dayton A, et al. Safe and targeted anticancer efficacy of a novel class of antioxidantconjugated difluoro-diarylidenylpiperidones: Differential cytotoxicity in healthy and cancer cells. Free Radic Biol Med. 2010 (in press).
26. Injac R, Strukelj B. Recent Advances in Protection Against Doxorubicin-induced Toxicity. Technol Cancer Res Treat 2008;7:497–516. [PubMed: 19044329]
27. Santos NA, Bezerra CS, Martins NM, Curti C, Bianchi ML, Santos AC. Hydroxyl radical scavenger ameliorates cisplatin-induced nephrotoxicity by preventing oxidative stress, redox state unbalance, impairment of energetic metabolism and apoptosis in rat kidney mitochondria. Cancer Chemother Pharmacol 2008;61:145–155. [PubMed: 17396264]

28. Maliakel DM, Kagiya TV, Nair CK. Prevention of cisplatin-induced nephrotoxicity by glucosides of ascorbic acid and alpha-tocopherol. Exp Toxicol Pathol 2008;60:521–527. [PubMed: 18644706]
29. Conklin KA. Dietary antioxidants during cancer chemotherapy: impact on chemotherapeutic effectiveness and development of side effects. Nutr Cancer 2000;37:1–18. [PubMed: 10965514]
30. Samuni Y, Gamson J, Samuni A, et al. Factors influencing nitroxide reduction and cytotoxicity in vitro. Antioxid Redox Signal 2004;6:587–595. [PubMed: 15130285]
31. Mitchell JB, Krishna MC, Kuppusamy P, Cook JA, Russo A. Protection against oxidative stress by nitroxides. Exp Biol Med (Maywood) 2001;226:620–621. [PubMed: 11444094]
32. Kuppusamy P, Li H, Ilangovan G, et al. Noninvasive imaging of tumor redox status and its modification by tissue glutathione levels. Cancer Res 2002;62:307–312. [PubMed: 11782393]
33. Kuppusamy P, Wang P, Shankar RA, et al. In vivo topical EPR spectroscopy and imaging of nitroxide free radicals and polynitroxyl-albumin. Magn Reson Med 1998;40:806–811. [PubMed: 9840823]
34. Hankovzky HO, Hideg K, Lex L, Nitroxyls VII. Synthesis and Reactions of Highly Reactive 1-Oxyl-2,2,5,5-tetramethyl-2,5-dihydropyrrole-3-ylmethyl Sulfonates. Synthesis 1980:914–916.
35. Kalai T, Tong L, Balog M, Selvendiran K, Kuppusamy P, Hideg K. Synthesis of N-substituted 3,5-bis(arylidene)-4-piperidones with high antitumor and antioxidant activity. Bioorg Med Chem. 2010 (to be communicated).
36. Bromberg JF, Wrzeszczynska MH, Devgan G, et al. Stat3 as an oncogene. Cell 1999;98:295–303. [PubMed: 10458605]
37. Burke WM, Jin X, Lin HJ, et al. Inhibition of constitutively active Stat3 suppresses growth of human ovarian and breast cancer cells. Oncogene 2001;20:7925–7934. [PubMed: 11753675]
38. Duriez PJ, Shah GM. Cleavage of poly(ADP-ribose) polymerase: a sensitive parameter to study cell death. Biochem Cell Biol 1997;75:337–349. [PubMed: 9493956]
39. Deeb D, Jiang H, Gao X, et al. Curcumin [1,7-bis(4-hydroxy-3-methoxyphenyl)-1-6-heptadine-3,5-dione; C21H20O6] sensitizes human prostate cancer cells to tumor necrosis factor-related apoptosis-inducing ligand/Apo2L-induced apoptosis by suppressing nuclear factor-kappaB via inhibition of the prosurvival Akt signaling pathway. J Pharmacol Exp Ther 2007;321:616–625. [PubMed: 17289836]
40. Gadducci A, Cosio S, Muraca S, Genazzani AR. Molecular mechanisms of apoptosis and chemosensitivity to platinum and paclitaxel in ovarian cancer: biological data and clinical implications. Eur J Gynaecol Oncol 2002;23:390–396. [PubMed: 12440809]
41. Jung EM, Park JW, Choi KS, et al. Curcumin sensitizes tumor necrosis factor-related apoptosis-inducing ligand (TRAIL)-mediated apoptosis through CHOP-independent DR5 upregulation. Carcinogenesis 2006;27:2008–2017. [PubMed: 16613838]
42. Ivanov VN, Bhoumik A, Krasilnikov M, et al. Cooperation between STAT3 and c-jun suppresses Fas transcription. Mol Cell 2001;7:517–528. [PubMed: 11463377]
43. Kim KW, Mutter RW, Cao C, et al. Inhibition of signal transducer and activator of transcription 3 activity results in down-regulation of Survivin following irradiation. Mol Cancer Ther 2006;5:2659–2665. [PubMed: 17121912]
44. Nielsen M, Kaestel CG, Eriksen KW, et al. Inhibition of constitutively activated Stat3 correlates with altered Bcl-2/Bax expression and induction of apoptosis in mycosis fungoides tumor cells. Leukemia 1999;13:735–738. [PubMed: 10374878]
45. Metz S, Naeth G, Heinrich PC, Muller-Newen G. Novel inhibitors for murine and human leukemia inhibitory factor based on fused soluble receptors. J Biol Chem 2008;283:5985–5995. [PubMed: 18174171]
46. Ziegler DS, Kung AL. Therapeutic targeting of apoptosis pathways in cancer. Curr Opin Oncol 2008;20:97–103. [PubMed: 18043263]

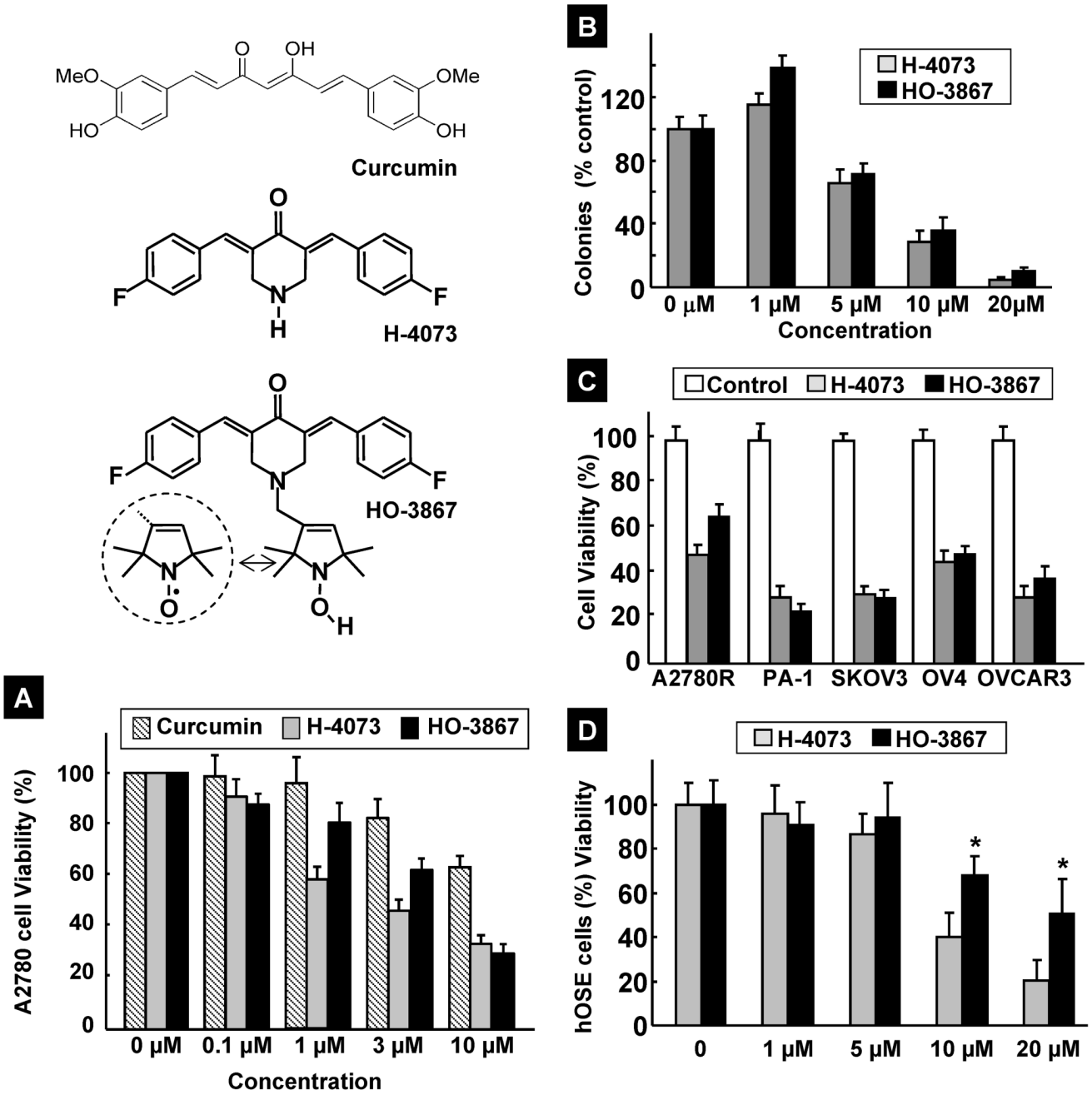

Figure 1. Inhibition of cell viability and proliferation by HO-3867

Structures of curcumin, H-4073, and HO-3867 are shown. H-4073 is a 3,5-diarylidenyl piperidone containing a *para*-fluoro substitution on the phenyl groups. HO-3867 contains an N-hydroxy-pyrroline moiety covalently linked to the N-terminus of piperidone. In aerated solutions and cells, the N-hydroxy-pyrroline undergoes conversion to, and exists in equilibrium with, the nitroxide (>NO) form (shown in the circle). (**A**) Dose-dependent effect of curcumin, H-4073, and HO-3867 on the viability of A2780 cells. Cells were incubated with curcumin, H-4073 or HO-3867 for 24 h followed by measurement of cell viability (by MTT assay). Values are expressed as mean ± SE (N=5). (**B**) Dose-dependent effect of H-4073 and HO-3867 on the colony-forming ability of A2780 cells. Values are expressed as mean ± SE (N=5). (**C**) Effect

of H-4073 and HO-3867 (10 μM; 24 h) on the viability of different ovarian cancer cell lines: A2780R (cisplatin-resistant variation of A2780), SKOV3, OV3, and OVCAR3. Values are expressed as mean ± SE (N=5). (**D**) Dose- and incubation-time dependent effect of HO-3867 (10 μM) on the viability of hOSE, a human ovary surface epithelial cell line used as a healthy control. Values are expressed as mean ± SE (N=5). *$p<0.05$ *versus* the effect of H-4073 at equivalent doses.

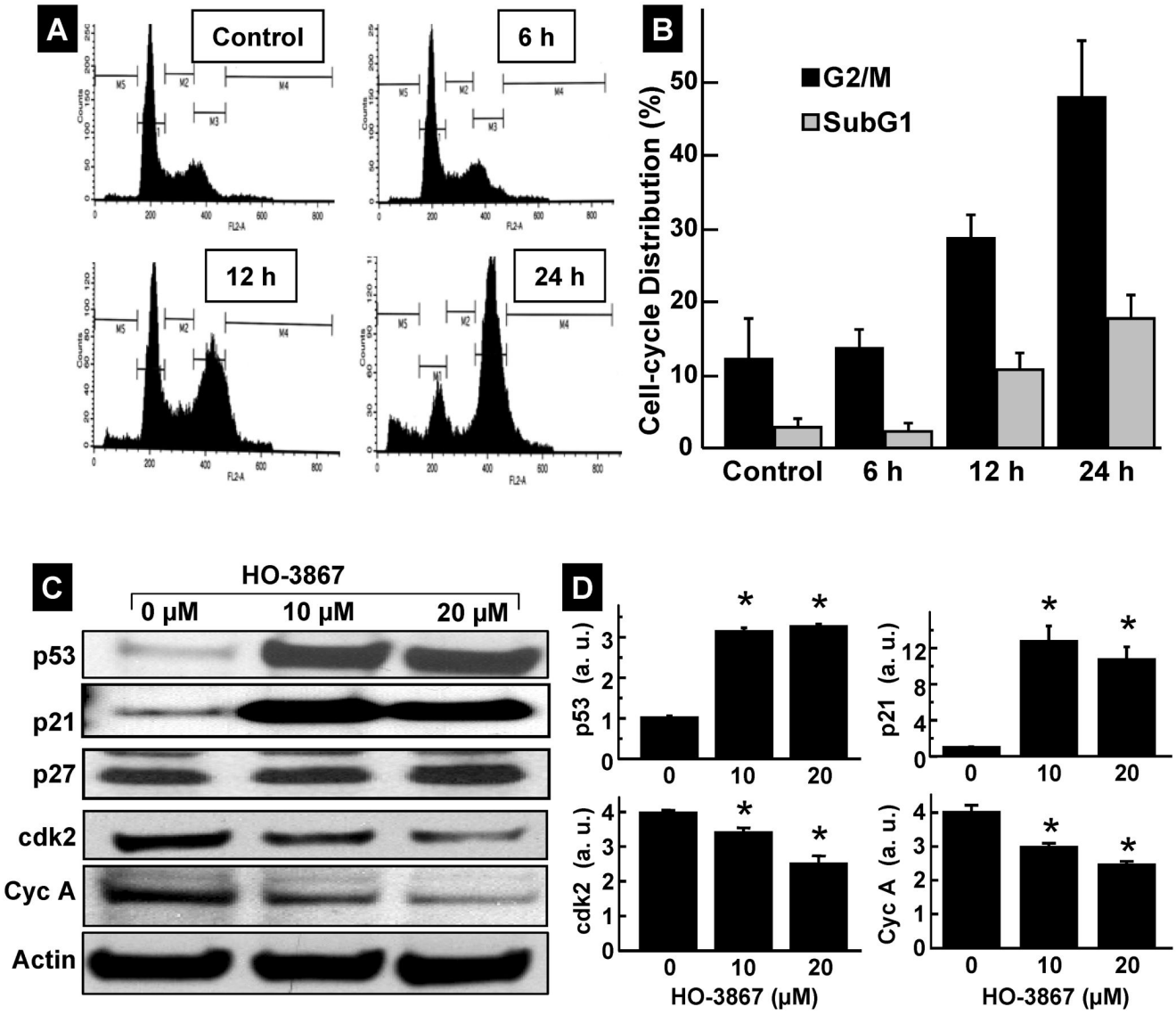

Figure 2. Modulation of cell-cycle progression and cell-cycle regulatory proteins by HO-3867

A2780 cells were treated with HO-3867 for 6 h, 12 h, or 24 h. (**A**) Representative flow cytometry profiles of control (0 μM) and HO-3867 (20 μM) treatment groups at different time periods. (**B**) Quantitative cell-cycle (DNA content) distribution (% of total) in the control and treatment groups. Data represent mean±SD (N=5) *p<0.01 *versus* Control. (**C**) Immunoblot images of cell-cycle regulatory proteins. (**D**) Quantitative results of p53, p21, cdk2, and cyclin A bands. Data represent mean±SD (N=5), *p<0.01 *versus* control (0 μM).

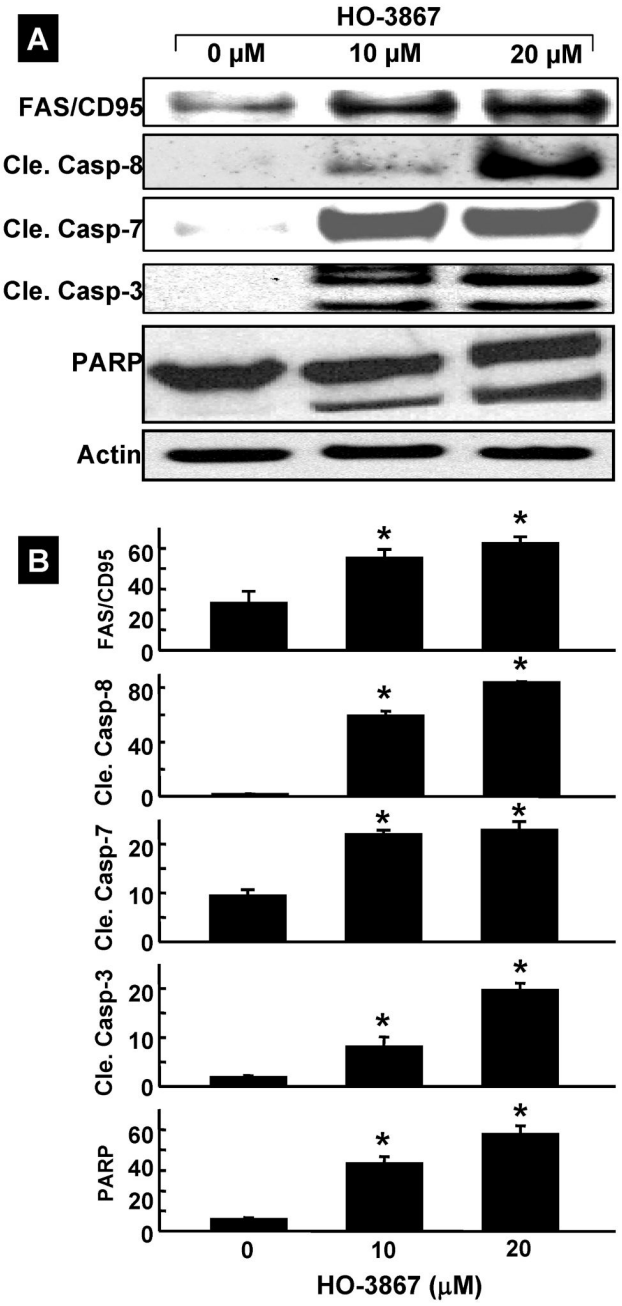

Figure 3. Induction of apoptosis by HO-3867

A2780 cells were treated with HO-3867 for 24 h and subjected to Western-blot analysis for apoptotic marker proteins. (**A**) Representative immunoblot images of FAS/CD95, cleaved caspases (8, 7, and 3), and PARP. (**B**) Quantitative results of immunoblot. Results are represented as mean±SD (N=5) expressed as arbitrary units, * $p<0.01$ *versus* control (0 μM).

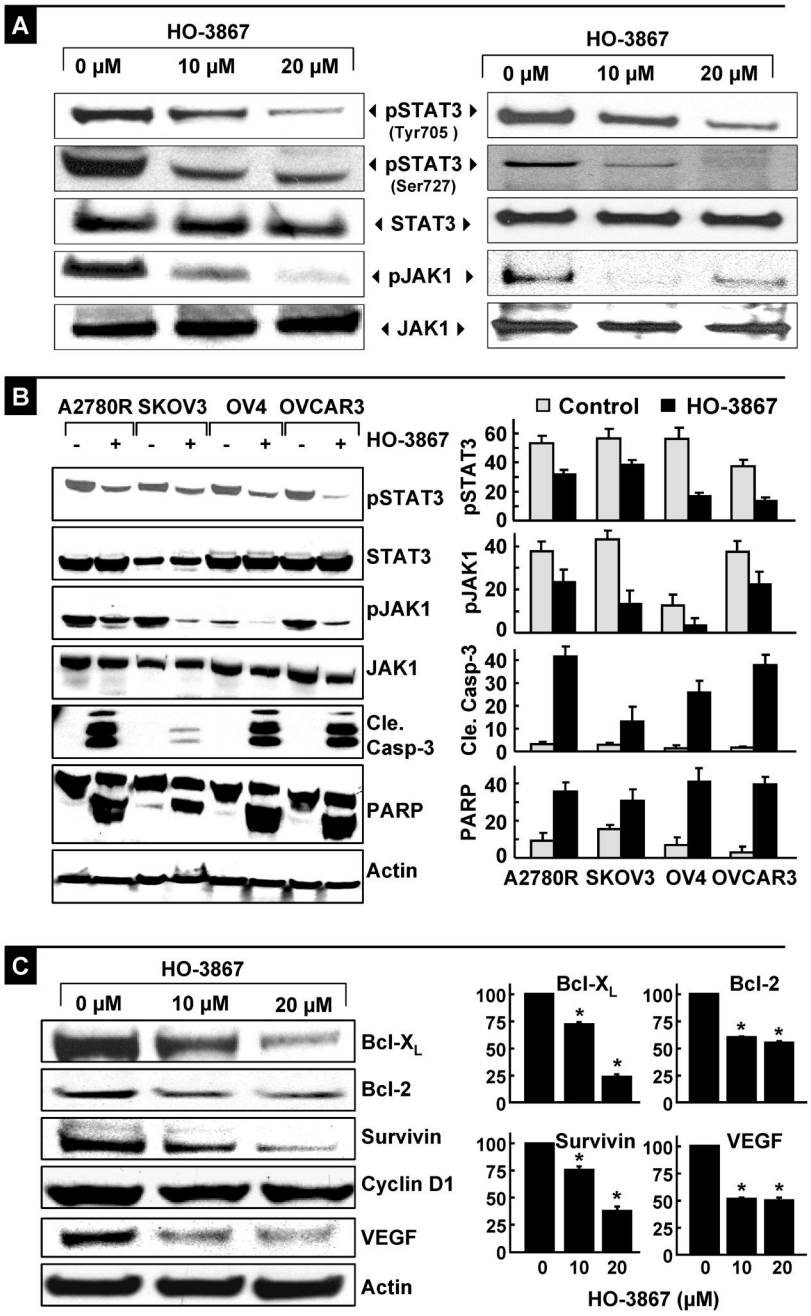

Figure 4. Inhibition of JAK/STAT3-signaling and downstream proteins by HO-3867

Cells were treated with H-4073 or HO-3867 for 24 h and subjected to Western-blot analysis. (**A**) Representative immunoblot images of phosphorylated and total STAT3 and JAK1 in A2780 cells and immunoprecipitation results of pSTAT3 (Tyr705/Ser727) and pJAK1 (Tyr1022/1023) using bands captured by STAT3 or JAK1 and blotted with pSTAT3 or pJAK1. (**B**) Representative Western blots obtained from four other ovarian cancer cell lines (A2780R, SKOV3, OV4, and OVCAR3) treated with 10-μM HO-3867 for 24 h. Note the decreased levels of pJAK1 and pSTAT3, and corresponding increased levels of cleaved caspase-3 and cleaved PARP in the treated cells compared to untreated cells. Densitometric analysis of Western blots are shown for pJAK1, pSTAT3, cleaved caspase-3 and cleaved PARP. Results are represented

as mean±SD (N=5) expressed as arbitrary units. (**C**) Immunoblot images of Bcl-xL, Bcl-2, survivin, cyclin D1, and VEGF proteins in cells. Quantitative results of Bcl-xL, Bcl-2, survivin, and VEGF bands are shown. Results are represented as mean±SD (N=5) expressed as a percent of control (*$p<0.01$).

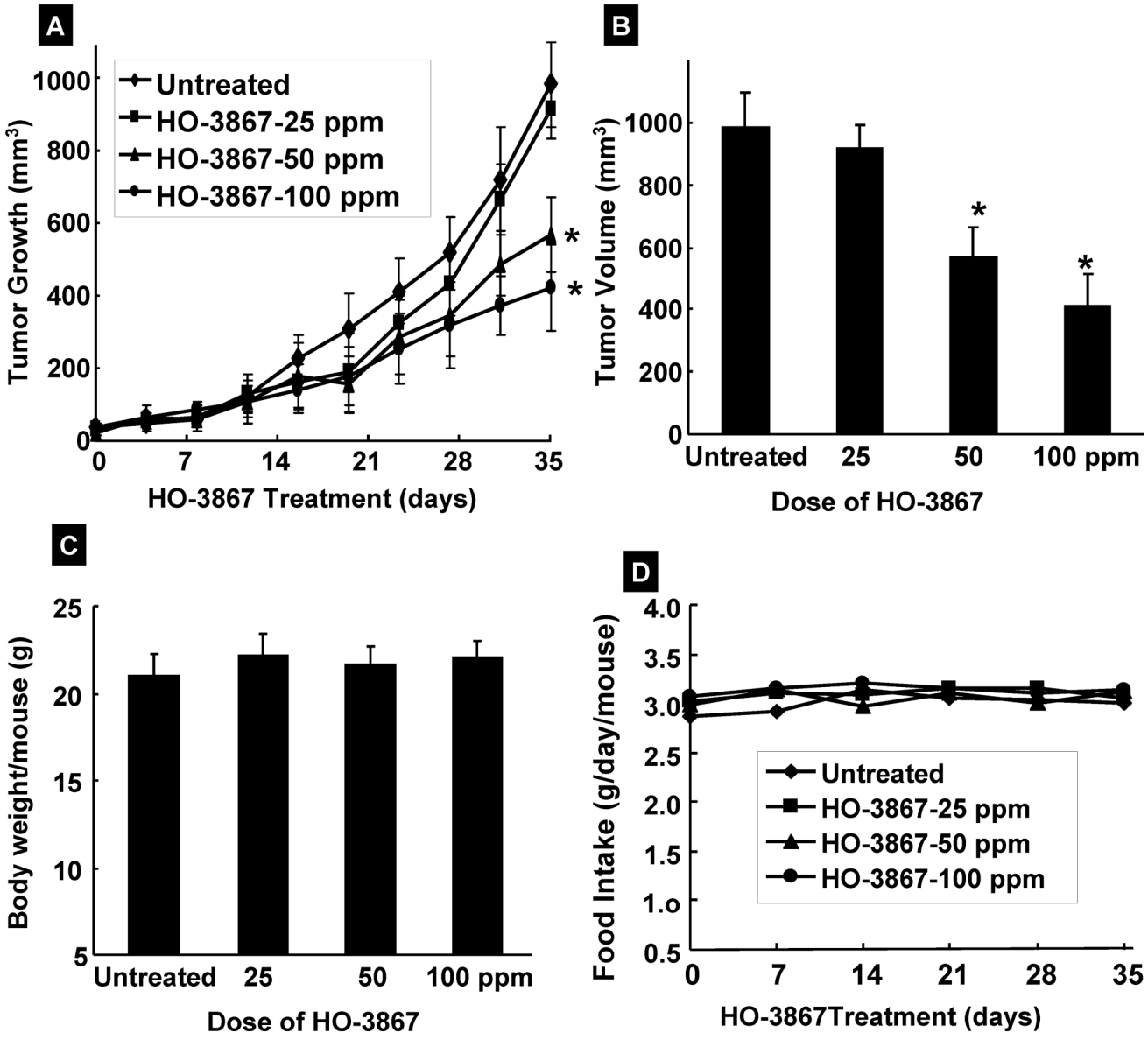

Figure 5. Effect of HO-3867 on murine xenograft tumors

(**A**) A dose-dependent decrease in the volume of the xenograft tumors growth is observed following HO-3867 treatment. (**B**) Final volume of HO-3867-treated tumors at the 5th week. (**C**) Change in body weight and (**D**) consumption of feed containing HO-3867 over time. Data represent mean±SE from 9 mice in each group. *p<0.05 *versus* untreated control group.

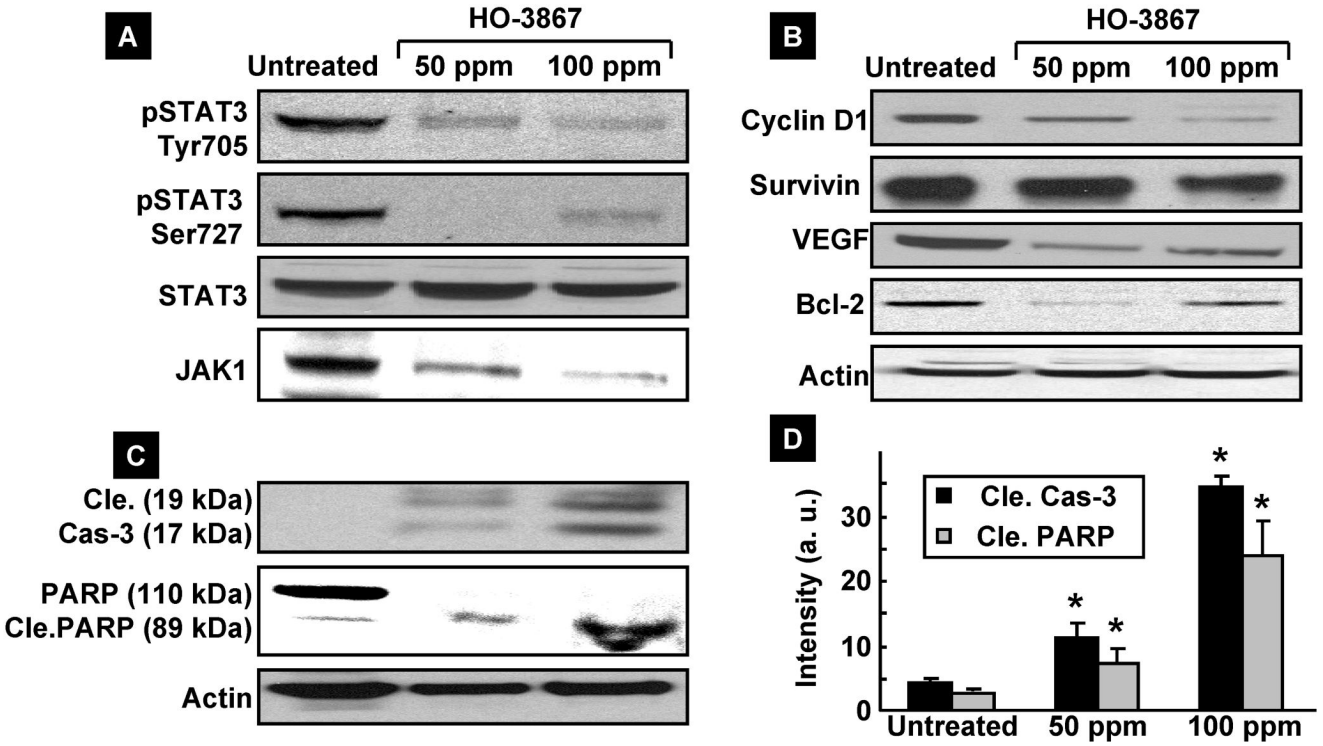

Figure 6. Effect of HO-3867 on the expression of JAK/STAT3 and targeting genes

(**A**) Immunoblot analysis using tissue lysates of xenograft tumors. The decreased expression of pSTAT3 Tyr705 and Ser727, and JAK1 are noted in the HO-3867-treated tumor lysates, in a dose-dependent manner, in concert with decreased expression of both Tyr705-phosphorylated and Ser727-phosphorylated STAT3. (**B**) The decreased expression is also shown in cyclin D1, Bcl-2 and VEGF in a dose-dependent manner. (**C**) Cleavage of caspase-3 and PARP in HO-3867-treated tumor lysates in a dose-dependent manner. (**D**) Quantification of cleaved caspase-3 and cleaved PARP. *p<0.05 *versus* respective untreated control group.